

A proper motion study of the Lupus clouds using VO tools

Belén López Martí¹, Francisco Jiménez-Esteban^{1,2,3}, and Enrique Solano^{1,2}

¹ Centro de Astrobiología (INTA-CSIC), Departamento de Astrofísica, P.O. Box 78, E-28261 Villanueva de la Cañada, Madrid, Spain
e-mail: belen@cab.inta-csic.es

² Spanish Virtual Observatory, Spain

³ Saint Louis University, Madrid Campus, Division of Science and Engineering, Avenida del Valle 34, E-28003 Madrid, Spain

Received; accepted

ABSTRACT

Context. The Lupus dark cloud complex is a well-known, nearby low-mass star forming region, probably associated with the Gould Belt. In recent years, the number of stellar and substellar Lupus candidate members has been remarkably increased thanks to the *cores to disks (c2d) Spitzer* Legacy Program and other studies. However, most of these newly discovered objects still lack confirmation of their membership to the dark clouds.

Aims. By using available kinematical information, we want to test the membership of the new Lupus candidate members proposed by the *c2d* program and by a complementary optical survey. We also plan to investigate the relation between the proper motions and other properties of the objects, in order to get some clues about their formation and early evolution.

Methods. We compile a list of members and candidate members of Lupus 1, 3 and 4, together with all available information on their spectral types, disks and physical parameters. Using Virtual Observatory tools, we cross-match this list with the available astrometric catalogues to get proper motions for our objects. Our final sample contains sources with magnitudes $I < 16$ mag and estimated masses $\geq 0.1 M_{\odot}$.

Results. According to the kinematic information, our sources can be divided into two main groups: The first one contains sources with higher proper motions in agreement with other Gould Belt populations, and whose spatial distribution, optical and near-infrared colours and disk composition are all consistent with these objects belonging to the Lupus clouds. In the second group, sources have lower proper motions with random orientations and they are mostly located outside the cloud cores; hence, their association with the Lupus complex is more doubtful. We investigate the properties of the higher proper motion group, but cannot find any correlations with spatial location, binarity, the presence of a circumstellar disk, or with physical properties such as effective temperature, luminosity, mass or age.

Conclusions. We conclude that the lower proper motion group probably represents a background population or mixture of populations unrelated to the Lupus clouds. The higher proper motion group, on the other hand, has properties consistent with it being a genuine population of the Lupus star forming region. More accurate proper motions and/or radial velocity information are required for a more detailed study of the kinematic properties of the Lupus stellar members.

Key words. stars:low-mass, brown dwarfs – stars: formation – stars: pre-main sequence – stars: luminosity function, mass function – astronomical database: miscellaneous – virtual observatory tools

1. Introduction

The Lupus dark cloud complex consists of six molecular clouds, named Lupus 1 to 6 (Tachihara et al. 1996, 2001). In terms of angular extent, it is one of the largest low-mass star forming complexes in the sky (nearly 20° across, with galactic longitudes $334^{\circ} < l < 352^{\circ}$ and latitudes $5^{\circ} < b < 25^{\circ}$), and it contains one of the richest associations of T Tauri stars (TTS). The clouds are projected against the Scorpius-Centaurus OB association, a vast complex at an average distance of about 140 pc from the Sun. This is one of the main structures of the Gould Belt, a young, expanding ring-like arrangement of OB associations, molecular clouds and other tracers of star formation that dominates the solar neighbourhood up to a distance of 600 pc (e.g. Comerón et al. 1994; Pöppel 1997). The estimated distance of 140-220 pc to the Lupus clouds matches well that of the Scorpius-Centaurus association, strongly suggesting a physical relationship between both entities.

The first studies of the stellar content identified at least 65 TTS within the complex, most of them classical T Tauri stars (CTTS), that is, young stars with indications of ongoing accretion in their spectra (e.g. Schwartz 1977; Krautter 1991; Hughes

et al. 1994). Later studies, the majority of them focused on the Lupus 3 cloud, used different techniques to increase the stellar and substellar census of the complex (e.g. Nakajima et al. 2000; Comerón et al. 2003; López Martí et al. 2005; Allen et al. 2007). A peculiarity of the Lupus region is that the distribution of stellar spectral types is dominated by M-type objects, in contrast to other low-mass star-forming regions (e.g. Appenzeller et al. 1983; Hughes et al. 1994; Wichmann et al. 1997a). The only exception are the two intermediate-mass Herbig Ae/Be stars HR 5999 and HR 6000 in the Lupus 3 cloud.

Three of the clouds, namely Lupus 1, 3 and 4, have been the target of *Spitzer* observations within the *Cores to Disks (c2d)* Legacy Program (Allers et al. 2006; Chapman et al. 2007; Merín et al. 2008). This study, one of the most comprehensive surveys in the complex, confirmed the youth of many previously suspected members of the region, and it also provided a list of about hundred low-mass candidate members based on the presence of excess in their spectral energy distributions (SEDs) at infrared wavelengths, where warm dust dominates the emission. Therefore, most of the objects presented by the *c2d* program

are surrounded by circum(sub)stellar disks and/or envelopes (so-called “class I and II sources”).

In a recent paper, Comerón, Spezzi & López Martí (2009, hereafter Comerón et al. 2009) reported on a broad-band optical (*RIz*) survey on the Lupus clouds with the WFI mosaic camera at the ESO/MPG 2.2m telescope on La Silla, complemented with *JHKs* photometry from 2MASS. In their surveyed areas, which overlap almost completely with the areas observed by the *c2d* program, they identify about 130 new low-mass candidate members of Lupus. Although their estimated ages are in the same range as the known members, these new candidate members are only moderately concentrated towards the dark clouds, and very few of the objects show infrared excess (that is, they are mostly so-called “class III sources”). Thus, the discovery of this new population poses interesting questions about the origin and early evolution of the stellar content of the Lupus complex as a whole. Comerón et al. analysed several possible formation scenarios that may have led to the observed populations. They also widely discussed the probability that the new diskless candidate members belong to an unrelated foreground population associated with the Gould Belt, which they held as unlikely given their apparent association with the dark cloud cores.

Kinematic information can help to shed more light on this issue, by providing further evidence of the membership of these objects to the same clustered structure as the known Lupus members. Moreover, the kinematic properties of the members of a given region or association hold important clues about its history. Some formation models predict that the early dynamical evolution of the parent proto-stellar cluster should lead to mass-dependent kinematic distributions (Kroupa & Bouvier 2003), while other numerical simulations predict similar kinematic properties over the whole mass spectrum (Bate et al. 2003; Bate 2009). A number of surveys have used proper motions to identify and confirm new low-mass members in young associations and clusters (e.g. Moraux et al. 2001; Kraus & Hillenbrand 2007; Bouy & Martín 2009; Caballero 2010), and various authors used radial velocity measurements to study the kinematic properties of young low-mass objects (e.g. Joergens & Guenther 2001; Joergens 2006; Jeffries et al. 2006; Maxted et al. 2008).

In this paper, we make use of proper motions from astrometric catalogues and of Virtual Observatory¹ (VO) tools to investigate the kinematic properties of the Lupus members and candidate members. Our goals are to provide further evidence for a common origin of all these objects, to test their association with the Lupus dark clouds, and to look for correlations between the proper motions and other physical properties of the objects, aiming at a better understanding of the formation of the stellar and substellar population within the Lupus complex.

2. Proper motions of Lupus members and candidate members

Our Lupus candidate members are the YSOs in Lupus 1, 3 and 4 provided by the *c2d* program (Merin et al. 2008) and the diskless cool stars identified in the optical WFI survey by Comerón et al. (2009). We also incorporated the previously known members of these clouds from the recent review by Comerón (2008). The three catalogues were cross-matched to avoid repeated entries and joint to produce a single catalogue for the complex. Table 1 gives the number of objects provided by each work. The compiled lists included 90, 208 and 33 objects in Lupus 1, 3 and 4, respectively, making 331 in total. We note that most of these

Table 1. Number of objects in each catalogue

Catalogue	Lupus 1	Lupus 3	Lupus 4	All
Previous	13	43	9 ^(a)	65
<i>c2d</i>	17	124	18	159
WFI	65	72	6	143
Compiled ^(b)	90	208	33	331
USNO-B1	30	55	8	93
SSS	80	163	23	266
PPMX	28	21	2	51
UCAC3	69	96	13	178

Notes.

^(a) Comerón (2008) erroneously lists as Lupus 4 members six objects actually belonging to the Norma 1 cloud, which are not considered in the present work.

^(b) Objects included in several catalogues have been counted once.

sources still lack spectroscopic confirmation of their youth and membership to the Lupus complex.

To get proper motion measurements of the Lupus candidate members, we cross-matched the merged catalogue with four astrometric catalogues which are available within the VO. These catalogues were the USNO-B1 (Monet et al. 2003), the SuperCOSMOS Sky Survey (SSS) (Hambly et al 2001), the Positions and Proper Motions-Extended (PPMX) catalogue (Röser et al. 2008), and the Third US Naval Observatory CCD Astrograph Catalog (UCAC3) (Zacharias et al. 2010). We took advantage of VO tools for this task. VO is a project designed to provide the astronomical community with the data access and the research tools necessary to enable the exploration of the digital, multi-wavelength universe resident in the astronomical data archives. In particular, to perform our cross-match, we made use of the Multiple Cone Search utility of TOPCAT², an interactive graphical viewer and editor for tabular data that allows the user to examine, analyse, combine and edit astronomical tables.

A matching radius of 2'' was used for all the catalogues, chosen after checking different values (1'', 2'', 3'', 10'') and finding 0.7'' and 0.4'' for the average separation and standard deviation, respectively, in the worst case. After this step, we retained all sources whose proper motion errors were not set to zero and had been computed using more than two epoch positions, and in the case of UCAC3 with object classification flag (ot) lower than 3, meaning it is a good star. After purging the data, the number of counterparts with proper motion data in USNO-B1, SSS, PPMX, and UCAC3 were 93, 266, 51, and 178, respectively. Table 1 gives the number of objects with valid counterparts in each Lupus cloud.

We compared the results of the cross-match with each catalogue. Note that it is not possible to combine the data for the different astrometric catalogues because not all catalogues use the same reference system. After the comparison, we decided to use only the data provided by UCAC3 in the general analysis, for the following reasons: USNO-B1 did not provide proper motions lower than 6 mas/yr; due to its lower sensitivity, the number of counterparts found in PPMX is very low compared to UCAC3 or SSS; and in the case of SSS, although it provided the largest number of counterparts, the typical error of the proper motions is about twice the typical error of UCAC3. Thus, UCAC3 provided us with a large data set, which has a suitable cover in proper motion and with reasonable errors for our study. Therefore, only the UCAC3 data will be considered in the following.

¹ <http://www.ivoa.net>

² <http://www.star.bris.ac.uk/~mbt/topcat/>

The UCAC3 catalogue is an all-sky survey containing about 100 million objects, 95% of them with proper motions, covering a dynamical range of 8-16 mag in the R band. Its positional accuracy is about 15 to 100 mas per coordinate, depending on magnitude. The proper motion errors range from 1 to 10 mas/yr, depending on magnitude and observing history; however, some systematic errors may be present in the proper motions of stars with $R \geq 14$.

Our final sample has 178 sources, the vast majority of them in Lupus 1 and 3. They correspond with the 77%, 46%, and 39% of the total number of sources included in our compiled lists of Lupus 1, 3, and 4, respectively.

3. Kinematic groups towards the Lupus clouds

The left panel of Fig. 1 shows the vector point diagram for the sources included in the UCAC3 astrometric catalogue. We clearly see two distinct groups, which are associated to the two peaks seen in the proper motion distribution (right panel): The first group (“Group A” in the following) is formed by sources with higher proper motions, the mean value being around $\mu \sim 28$ mas/yr; while the objects belonging to the second group (“Group B”) have lower proper motions, with a mean close to $\mu \sim 8$ mas/yr.

We carefully checked the reliability of the two groups making use of all the information provided by the UCAC3 catalogue. We did not find any photometric bias nor any particular flag or warning suggesting that one of the groups could be spurious or of worse quality than the other. Therefore, according to the UCAC3 data both groups are equally reliable. Moreover, because both groups are also recognized in the three clouds separately (in Lupus 4 less clearly due to the low number of sources), they do not seem to be related to any particular cloud, but rather to the Lupus sky area as a whole.

As a further check, we created vector point diagrams using the data from USNO-B1, SSS, and PPMX. A detailed comparison between these diagrams, taking into account the different errors and sensitivities of the data sets, shows a very good agreement.

The conclusion is that both Group A and B are probably real, that is, that the Lupus members and candidate members can be divided into two main populations. We list the objects belonging to each of these groups in Tables 2 and 3. The nature of these populations and their relation to the Lupus dark clouds is discussed in Sect. 4.1 below.

There are sources whose proper motion components make their location in the vector point diagram compatible, within the given errors, with either of the groups. These ambiguous cases are labeled in Tables 2 and 3. We also identify a number of sources with clearly discrepant proper motions, which are discussed in the Appendix A.

4. Analysis and discussion

4.1. Origin of the kinematic groups

In order to clarify their origin and relation to the Lupus complex, we carefully analysed the properties of the sources included in Groups A and B. Figs. 2 to 4 show the current spatial location of the sources included in the UCAC3 catalogue and their expected displacement within 10^5 Myr. We see that most of the Group A sources have similar proper motion directions (towards the South-West), suggesting a common origin. The Group B sources, on the other hand, exhibit a variety of proper motion

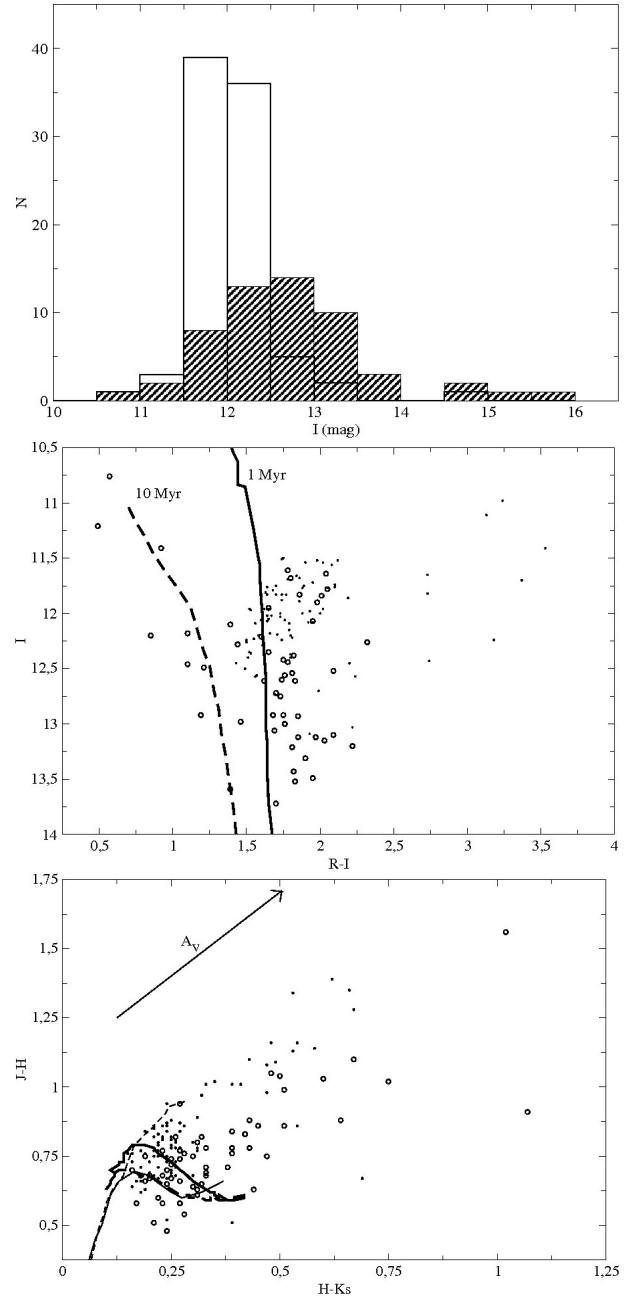


Fig. 5. Photometric properties of the Lupus members and candidate members. *Upper panel:* I -magnitude distribution for Groups A and B (filled and blank histogram, respectively). *Middle panel:* $(I, R - I)$ colour-magnitude diagram for the Lupus objects. Group A and Group B sources are indicated with open circles and dots, respectively. The thick solid and dashed lines are the 1 and 10 Myr isochrones, respectively, from the models by Baraffe et al. (1998). *Lower panel:* $(J - H, H - K_s)$ colour-colour diagram for the Lupus objects. The thin dashed and solid lines correspond to the giant and dwarf loci, respectively, from Bessell & Brett (1988). An extinction vector of 5 mag according to the law by Cardelli et al. (1989) is also indicated. Other symbols as in the previous panel.

directions, in the majority of cases totally discrepant with the one followed by Group A. This suggests that Group B may be formed by populations of various origins.

In Lupus 3, we also see differences in the spatial distribution of the sources: The objects in Group A tend to be more concentrated towards the cloud core than the objects in Group B, which

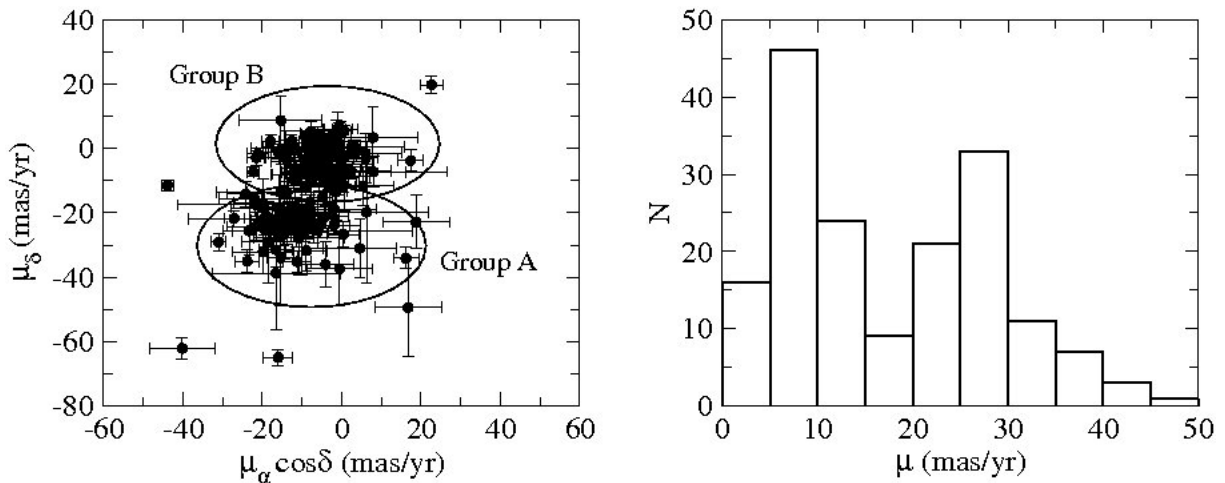


Fig. 1. Vector point diagram (left panel) and proper motion histogram (right panel) for the Lupus sources included in the UCAC3 catalogue. A few sources with very large proper motion have not been plotted (see Table A).

tend to avoid the densest areas of the cloud. Outside the core, however, the distributions of both groups are indistinguishable. These differences in spatial distribution are not evident, however, in either of the other two clouds.

Most of the Lupus members confirmed spectroscopically belong to Group A, because the majority of studies have focused on the cloud cores. The only exceptions are Par-Lup3-2 (M6) and Sz 105 (M4), both in Lupus 3, which seem to belong to Group B, although their locations in the vector point diagram are not very far from the Group A sources.³

It is also noteworthy that Group B seems to be composed almost exclusively by diskless stars (class III sources) according to the literature (Merín et al. 2008; Comerón et al. 2009). The only exceptions are 160708.6-394723 and 161148.7-381758, which seem to harbour accretion disks (they are class II sources). On the contrary, Group A includes both stars with and without disks (see discussion in Sect. 4.3.3). This suggests that Group B represents, as a whole, a later evolutionary stage than Group A, since disks are expected to be found around newly formed stars and to dissipate with time.

The optical and near-infrared photometry provided by Merín et al. (2008) and Comerón et al. (2009) can help to clarify the nature of Group B. As shown in the upper panel of Fig. 5, this group represents, as a whole, a brighter sample than Group A, which includes a significant amount of sources with $I > 12$ mag. However, for similar I magnitudes, the Group B stars tend to have redder $R-I$ colors, as seen in the $(I, R-I)$ colour-magnitude diagram (central panel of Fig. 5), a fact that suggests higher extinction. Finally, in the near-infrared colour-colour diagram (lower panel of Fig. 5) we see that, with a couple of exceptions, the Group B sources tend to be located along the reddening band for giants, although this locus can also be occupied by reddened young stars of late K and early M spectral types. The Group A sources, on the other hand, have colours more consistent with reddened mid-to-late M-dwarfs or young stars with near-infrared excess.

All these facts (lower proper motions, different proper motion directions, virtual lack of sources with disks, optical and near-infrared colours) strongly suggest that Group B represents

a population (or a mixture of populations) located behind the dark clouds, and probably unrelated to the complex. The true nature of these objects cannot be discerned with the optical and infrared photometry alone, and needs to be clarified with spectroscopy. Group A, on the other hand, has properties consistent with it being a genuine population of the Lupus star forming region.

4.2. Comparison to other populations

In an attempt to throw more light on the origin of the two kinematic groups identified towards the Lupus clouds, and their relationship to larger structures, we compared their proper motions with those of other Gould Belt populations. Like in the case of Lupus, we performed a Multiple Cone Search in the UCAC3 catalogue to get proper motion measurements for these comparison objects. Fig. 6 shows again the vector point diagrams for the Lupus sources, where we have overplotted the objects from the populations discussed below.

4.2.1. ROSAT pre-main sequence stars in the area of the Lupus clouds

Krautter et al. (1997) reported on the discovery by the ROSAT X-ray satellite of an extended population of weak-lined T Tauri stars (WTTS) towards the Lupus clouds, which greatly exceeds in number the CTTS population coincident with the cloud cores. Some of these WTTS are seen projected onto regions of high obscuration, while others are located far from the cloud cores. In addition, the estimated age of this dispersed population is older than that of the previously known Lupus stellar members. Wichmann et al. (1997b) argued that the age (up to $5-6 \cdot 10^7$ yr) and spatial distribution of the ROSAT stars are consistent with their belonging to the Gould Belt rather than to the Lupus clouds themselves, whose mean age is estimated to be around 5 Myr.

The UCAC3 catalogue contains counterparts for 91 of the 136 ROSAT stars from Krautter et al. (1997). These sources are, with a few exceptions, located in the same area as Group A in the vector-point diagram of Fig. 6, a fact that suggests that both populations may have a similar origin. Only six ROSAT stars are seen detached from this group, and a couple of them, namely RXJ1506.9-3714 and RXJ1605.5-3846, are located in the Group B area.

³ We note that Sz 105 has a known companion (Ghez et al. 1997) at $\sim 10''$, which is also included in UCAC3 (source 100-192094). The average proper motion of both sources has values consistent with membership to Group B.

4.2.2. Members of the Upper Scorpius association

The Upper Scorpius (USco) OB association belongs to the largest Scorpius-Centaurus structure within the Gould Belt. Thus, it is located not far from the Lupus clouds. Over the last decade, it has been one of the most targeted star forming regions for the search and study of low-mass stars and very low-mass objects. Combining samples of USco members from the literature, Bouy & Martín (2009) recently performed a kinematic study of the low-mass population in this region using the USNO-B1 and UCAC2 catalogues. We performed the Multiple Cone Search in the UCAC3 catalogue using the same compiled list as these authors, kindly provided to us by H. Bouy. It is important to note that all the sources studied by Bouy & Martín (2009) have spectroscopic confirmation of youth.

The USco UCAC3 sample contains 129 of the 514 objects in the list of Bouy & Martín. In Fig. 6 we see that the majority of them are coincident in proper motion with our Group A sources, again suggesting a similar origin. Nonetheless, nine stars have proper motions that seem to be in agreement with Group B. Of them, one star, USco J161026.4-193950, had been identified as a kinematic member of Upper Scorpius by Bouy & Martín (2009). Another source, USco J155744.9-222351, is classified as an outlier by these authors. The remaining objects (UScoCTIO 31, UScoCTIO 36, USco J160132.9-224231, USco J160545.4-202308 and USco J161021.5-194132) do not have available proper motions in the work by Bouy & Martín (2009).

In summary, the proper motions of the Group A sources are in full agreement with those of other Gould Belt populations, a fact that reinforces the idea that this group, and hence the Lupus dark cloud complex, is associated to this large structure. A few stars from other Gould Belt structures have similar proper motions to those of the Group B sources; however, they are very few, and without further information (e.g. radial velocities), we cannot rule out that this coincidence is just a matter of chance due to the projection of their true spatial motions on the sky.

4.3. Properties of the Lupus kinematic members

Our kinematic analysis has shown that the sources in Group A are likely to be members of the Lupus star forming region, while Group B seems to represent a background population. In particular, about one third of the Group A sources have been spectroscopically confirmed as pre-main sequence stars. The definitive confirmation of youth for the rest of the objects needs to await for spectroscopy; nonetheless, due to the good agreement of their proper motions with those of the confirmed members, we expect contamination to be minimal.

In the following discussion, we thus consider all the stars in Group A, and only the stars in that group, as probable Lupus members. This group contains 75 stars, of which 25 have spectroscopic confirmation of their status. Note that the embedded and/or highly extincted population, as well as the lowest-mass members of the Lupus complex ($M < 0.1M_{\odot}$), are certainly missing in this sample, due to the relatively bright magnitude limit of the astrometric catalog.

4.3.1. Spatial location

As shown in Figs. 2 to 4, the Group A sources (our Lupus kinematic members) exhibit similar proper motions in all three clouds, as expected if these clouds belong to the same large structure. Moreover, these sources can be divided into two samples according to their spatial location: a first, more numerous group of objects that are seen concentrated towards the cloud cores, and a second group of stars which are dispersed around the densest cloud areas. However, no evident difference is seen between the in- and the off-cloud population, neither in proper motion moduli nor in proper motion direction. This seems to confirm that both samples belong to the same structure. It also suggests that the location of the outer sources is not the consequence of these objects being ejected from their parental birth sites.

Two stars (Sz 92 and SSTc2d J160734.3-392742) seem to be moving differently in Fig. 3, as though they were escaping from the Lupus 3 cloud. These sources are located to the right edge of the Lupus group in the vector point diagram, slightly detached from the rest (see left panel of Fig. 7). We could restrict our selection in the vector point diagram to avoid these runaway sources; however, the fact that one of them (Sz 92) has been confirmed spectroscopically as a member of Lupus suggests that their discrepant proper motions may have a different cause rather than non-membership. Dynamical interactions with other cloud members or unresolved binary companions may be responsible for the measured discrepant proper motions. Given the large errors, it is also possible that more accurate measurements are able to reconcile their proper motions with those of the majority of Lupus members.

4.3.2. Binarity

Since the presence of unresolved nearby sources in the images used for the construction of the UCAC3 catalogue can affect the proper motion measurements, we checked the binarity of our probable Lupus members. Our sample includes 12 reported visual binaries and one triple system, Sz 130 (Reipurth & Zinnecker 1993; Ghez et al. 1997; Merín et al. 2008). They are labeled in Table 2. We do not find any relation between the presence of a companion and the proper motion modulus or direction of the system; in other words, not all the discrepant objects are known multiple systems, nor all known multiple systems have discrepant proper motions.

We note that the separation of the reported companions is relatively large (between 1 and 10'', except for Sz 74, whose companion is located at 0.24''), as most of them have been identified in visual searches. To date, the vast majority of companions still lack confirmation of their youth and membership to the Lupus clouds. We tried to throw more light on this issue by looking for proper motion measurements for these companions in UCAC3. However, due to their faintness, they are not included in this catalogue. The only exception is the reported companion to Sz 91 in Lupus 3, for which we find a possible counterpart at 8.3'' to the South-East (UCAC3 102-194472, $\mu_{\alpha} \cos \delta = 12.1$ mas/yr, $\mu_{\delta} = -40.6$ mas/yr). The proper motion of the combined system looks compatible with its belonging to the Lupus kinematic group.

4.3.3. Stars with and without disks

According to the analysis of their spectral energy distributions (SEDs) performed by Merín et al. (2008) and Comerón et al.

(2009), our UCAC3 sample contains 36 stars with disks (class II sources) and 37 diskless stars (class III sources), as well as one star thought to possess a disk and a circumstellar envelope (a class I source), namely Sz 102 in Lupus 3. Another source (160836.2-392302, also in Lupus 3), could be in an intermediate state between class I and II (Comerón et al. 2009), but it will be considered a class II source in the following. According to these numbers, the disk fraction in our kinematic member list is about 50%, lower than the 70-80% estimated by Merín et al. (2008) in their *c2d Spitzer* survey. Although this could suggest that our sample is incomplete in terms of disks, we note that a significant fraction of the diskless stars in our sample come from the survey by Comerón et al. (2009), which was published after Merín et al.'s study. Our estimated disk fraction is in any case within the range observed in other star forming regions of similar ages (Haisch et al. 2001; Mamajek 2009), so we believe it is quite representative of the disk composition of the Lupus population down to about $0.1M_{\odot}$ (corresponding to $I \sim 14.5$ mag at the age and distance of the Lupus clouds, according to Baraffe et al. 1998).

We searched for correlations between the existence of a disk and the proper motion properties of the objects. In Fig. 7, we show the vector-point diagram and the total proper motion histograms for the objects in our member list, divided by SED class (class I and II versus class III). The proper motions of class I-II and class III are indistinguishable with the available data.

As already reported by previous authors (e.g. Hughes et al. 1994; Merín et al. 2008; Comerón et al. 2009), most of the objects located outside the cloud cores are diskless stars, and thus theoretically more evolved than the in-cloud population, which consists mainly on stars with disks. However, the estimated ages of both groups are similar (Comerón et al. 2009). A possible explanation for the apparently faster evolution of the off-cloud population would be that these sources had been ejected from their parental birth sites, hence being devoid of circumstellar material to accrete. However, as stated in Sect. 4.3.1 above, the fact that the proper motions of these sources are very similar to those of the in-cloud population seems to contradict this picture. Comerón et al. (2009) proposed that the off-cloud population formed after the passage of one or more shock fronts associated with evolved supernova remnants, triggering the collapse of pre-existing cloudlets. The outside-in collapse produced by this scenario, as opposed to the inside-out collapse of the cores embedded in the clouds, may explain the different disk properties of both populations. Another alternative explanation would be the dissipation of unshielded disks by the ultraviolet radiation of O-stars from the Scorpius-Centaurus OB association, but this mechanism is more doubtful given the distance of the association to the Lupus clouds.

4.3.4. Spectral types and physical parameters

Spectral types are related to the effective temperature of the objects and, in the case of PMS stars, they are also directly related to the mass. Bouy & Martín (2009) investigated the relation between proper motion and spectral type for their sample of Upper Scorpius members, and found no correlation between these parameters. We now attempt to make a similar check with our Lupus kinematic members.

As mentioned previously, only 25 objects in our member list have spectral types available in the literature. Except for three K-type stars (Sz 102, Sz 133 and Sz 118), they span the range M0-M6, often with only two or three objects in each subclass.

In order to increase our sample, we made use of effective temperatures instead of spectral types. The temperatures were estimated in two different ways: For those sources with published spectral types, we transformed the spectral types into temperatures using the scale by Luhman et al. (2003). Since some authors (e.g. Barrado y Navascués et al. 2004) have found discrepancies of up to 200 K between the Luhman scale and other temperature estimations, we consider an error of 200 K for these T_{eff} values. For the rest of sources, we directly took the effective temperatures provided by Comerón et al. (2009; see their Tables 4 and 9), derived by fitting the SEDs of the objects using model spectra from Hauschildt et al. (1999) and Allard et al. (2000). For $T_{eff} < 4000$ K, these authors again estimate an error of ± 200 K in their temperature values. We note that the Luhman scale was set to be compatible with the Baraffe et al. (1998) evolutionary models, based on the same atmospheric models used by Comerón et al. for their SED fitting.

It is important to remark that Comerón et al. only attempted to fit the stellar photospheres of the objects, thus assuming any contribution from the disk or the accretion to the total flux to be negligible. As a consequence, their fits are less reliable for stars with strong accretion and/or high near-infrared excesses; indeed, Comerón et al. (2009) caution that, in such cases, too high effective temperatures and extinctions are derived. The number of stars in our member list with reliable fits in that work is 28 (twenty diskless stars and eight stars with disks), of which 10 have published spectral types. Hence, we have effective temperatures derived from the SED fitting for 18 objects, most of them class III sources. Together with the 25 stars with spectral types, this makes a sample of 43 sources. The estimated effective temperatures range between 5000 and 3000 K, with a majority of stars having $T_{eff} < 4000$ K, as expected for M-type objects.

Fig. 8 shows the proper motion components of our objects plotted against effective temperature. The plots show no correlation between these parameters. No clear trend is seen either when stars with and without disks are considered separately.

Using the parameters from the SED fitting, Comerón et al. (2009) also derived absolute luminosities, masses and ages for the objects from the evolutionary models by Baraffe et al. (1998) and Chabrier et al. (2000). They assumed a distance of 200 pc to the complex. According to their results, the 28 stars with reliable fits in our member list have masses between 0.1 and $1.4M_{\odot}$, luminosities in the range 0.08 - $1.1L_{\odot}$ (except for one object, Sz 118, with $L = 4.3L_{\odot}$) and estimated ages younger than 15 Myr. We used this subsample to look for correlations between the proper motions and the physical parameters of the objects. However, as shown in Fig. 9, no clear variations of the proper motions with luminosity, mass or age are seen. More accurate proper motion measurements would be required to reveal any eventual trend with the physical properties of our objects.

5. Conclusions

Our kinematical analysis of the Lupus members and candidate members has unveiled two main groups of sources. The first one, our Group A, has proper motions, spatial distribution and colours consistent with it being a genuine population of the star forming complex. Besides, we have shown that the proper motions of the sources in this group are consistent with those of other Gould Belt populations, thus reinforcing the idea of a physical connection between the dark clouds and this large structure. The second group, our Group B, has lower proper motions with random directions, and the sources in this group tend to avoid the location of the cloud cores. In addition, the optical and near-

infrared colours of these objects are consistent with them being reddened giants. All this suggests that Group B represents a background population or mixture of populations, probably unrelated to the Lupus clouds. However, the fact that a few spectroscopically confirmed members of Lupus and of other Gould Belt structures have locations in the vector point diagram that are consistent with Group B leaves open the possibility that this group may contain some other true Lupus members, but whose proper motions are, for some reason, discrepant respect to the majority of objects belonging to the complex.

We have investigated any possible relationship between the proper motions and other properties of these sources, such as spatial location, binarity, the presence of an accretion disk, and several physical parameters (effective temperature, luminosity, mass, age), but we have found no evident trends with the available data. In particular, we do not see differences between the objects located within the cloud cores and those located outside these cores. This suggests that the dispersed population has not been ejected from the densest cloud areas, but actually formed outside the cores. More accurate proper motions, hopefully combined with radial velocity information, can unveil any possible trend hidden to the precision of the proper motions used here, and will help to throw more light on the formation process of the stellar content of the Lupus clouds.

Our study has shown how the use of kinematical information can complement photometric data to constrain the selection of members of young star forming clusters, minimizing the contamination of the samples. Currently available astrometric catalogues are deep enough to provide proper motions for a significant number of candidate members of nearby star forming regions. Kinematic information can also help to better know the formation process of these objects, especially if it can be combined with physical parameters derived from SED fitting and/or spectroscopic data. The *Gaia* mission of the European Space Agency, whose launch is foreseen in 2012, will provide this information with unprecedented precision for most of the stars in the sample studied here, allowing a three-dimensional study of Lupus and other nearby star-forming regions.

Acknowledgements. We kindly thank H. Bouy, F. Comerón, B. Merín and J. A. Caballero for useful discussions. This work was funded by the Spanish MICINN through grant Consolider-CSD2006-00070. It also benefited from funding from the Spanish and Madrid regional governments through grants ESP2007-65475-C02-02 and PRICIT-S2009ESP-1496, respectively. This research has made use of the Spanish Virtual Observatory supported from the Spanish MEC through grant Aya2008-02156.

This publication greatly benefited from the use of the SIMBAD database and VIZIER catalogue service, both operated at CDS (Strasbourg, France). We used the VO-compliant tools Aladin, developed at CDS, and TOPCAT, currently developed within the AstroGrid project.

Appendix A: Outlier analysis

Some objects present proper motions which are clearly discrepant from those of the stars in Group A and B. In this Appendix, we discuss the reliability of the proper motion measurements for these objects, which are listed in Table A.

Initially, nine sources were identified as outliers in the vector point diagram: four in Lupus 1, four in Lupus 3, and one more in Lupus 4. To check the reliability of the reported proper motions, we visually inspected these objects with peculiar proper motion with Aladin. We compared and blinked two sets of images separated several decades in time, from the optical DSS-1 and the near-infrared 2MASS surveys, to easily confirm the high proper motion of our candidates. The 2MASS (Skrutskie

et al. 2006) sources and UCAC3 counterparts were superimposed on the images to assess the reliability of the cross-match. Besides, we used other available astro-photometric databases, such as the Astrographic Catalogue AC2000.2 (Urban et al. 1998), the SuperCOSMOS Sky Survey, the USNO-B Catalog and the PPMX catalogue, to verify the peculiar proper motions.

From the original group of nine sources, six turned out to have reliable proper motions that are discrepant from those of Groups A and B. Figs. 2 to 4 show their location and their expected displacement after 10^5 yr. Although most of the outliers are located outside the densest cloud areas, two stars (153940.8-333941 in Lupus 1 and 160908.5-390213 in Lupus 3) are seen towards the cloud cores. Note that the objects from Table A with wrong proper motions are not plotted in these figures.

The proper motion values and directions differ greatly among these sources. Three objects are seen not far, but clearly detached, from Groups A and B in the vector point diagram, having $\mu \lesssim 50$ mas/yr: 154344.5-335834 in Lupus 1 and 161001.1-384315 and Sz 95 in Lupus 3. We note that this latter star has a reported visual companion at a separation of $\sim 3''$ according to Comerón (2008), but this second object has no UCAC3 counterpart.

The remaining sources in the list of outliers have $50 < \mu < 100$ mas/yr, except for 154144.0-343530 in Lupus 1, which has an even larger value, $\mu \sim 270$ mas/yr. Such high proper motions suggest they might be foreground sources.

With a single exception (Sz 95), all these outliers are diskless stars according to the SED analysis (Merín et al. 2008; Comerón et al. 2009), a fact that is consistent with them belonging to the field. However, we note that ejected members from star forming regions are expected to possess only truncated disks, which would thus dissipate much faster than disks around the in-cloud population. Should some of them be members of the Lupus clouds, these objects would have masses around $0.3-0.4M_{\odot}$ according to the SED fitting results by Comerón et al. (2009), very close to the median mass of the stars in the region.

References

- Allard, F., Hauschildt, P. H. & Schwenke D. 2000, *ApJ* 540, 1005
 Allen, P. R., Luhman, K. L., Myers, P. C. et al. 2007, *ApJ* 655, 1095
 Allers, K. N., Kessler-Silacci, J. E., Cieza, L. A. & Jaffe, D. T. 2006, *ApJ* 644, 364
 Appenzeller, I., Jankivicks, I. & Krautter, J. 1983, *A&AS* 53, 291
 Baraffe, I., Chabrier, G., Allard, F. & Hauschildt, P. H. 1998, *A&A* 337, 403
 Barrado y Navascués, D., Mohanty, S. & Jayawardhana, R. 2004, *ApJ* 604, 284
 Bessell, M. S. & Brett, J. M. 1988, *PASP* 100, 1134
 Bate, M. R., Bonnell, I. A. & Bromm, V. 2003, *MNRAS* 339, 577
 Bate, M. R. 2009, *MNRAS* 392, 590
 Bouy, H. & Martín, E. L. 2009, *A&A* 504, 981
 Caballero, J. A. 2010, *A&A* 514, A18
 Cardelli, J. A., Clayton, G. C. & Mathis, J. S. 1989, *ApJ* 345, 245
 Chabrier, G., Baraffe, I., Allard, F. & Hauschildt, P. H. 2000, *ApJ* 542, 464
 Chapman, N. L., Lai, S.-P., Mundy, L. G. et al. 2007, *ApJ* 667, 288
 Comerón, F., Torra, J. & Gómez, A. E. 1994, *A&A* 286, 789
 Comerón, F., Fernández, M., Baraffe, I. et al. 2003, *A&A* 406, 1001
 Comerón, F. 2008, in Reipurth, B. (Ed.): *Handbook of Star Forming Regions*, Volume II, 295
 Comerón, F., Spezzi, L., & López Martí, B. 2009, *A&A* 500, 1045
 Ghez, A. M., McCarthy, D. W., Patience, J. L. & Beck, T. L. 1997, *ApJ* 481, 378
 Haisch, K. E., Lada, E. A. & Lada, C. J. 2001, *ApJ* 553, L153
 Hambly, N. C., MacGillivray, H. T., Read, M. A., et al. 2001, *MNRAS*, 326, 1279
 Hauschildt P. H., Allard F. & Baron E. 1999, *ApJ* 512, 377
 Hughes, J. D., Hartigan, P., Krautter, J. & Kelemen, J. 1994, *AJ* 108, 1071
 Jeffries, R. D., Maxted, P. F. L., Oliveira, J. M. & Naylor, T. 2006, *MNRAS* 371, L6
 Joergens, V. & Guenther, E. 2001, *A&A* 379, L9
 Joergens, V. 2006, *A&A* 448, 655

Table A.1. Outliers in the Lupus vector point diagram

SSTc2d J	Other names	α (J2000)	δ (J2000)	UCAC3	$\mu_\alpha \cos \delta$ (mas/yr)	μ_δ (mas/yr)	Notes
Lupus 1 cloud							
153928.3-344618		15:39:28.3	-34:46:18	111-179768	157.6 ± 5.6	-40.2 ± 5.6	1
153940.8-333941		15:39:40.8	-33:39:41	113-182897	-16.0 ± 3.7	-65.0 ± 2.5	
154144.0-343530		15:41:44.0	-34:35:30	111-180079	-255.7 ± 10.2	-87.8 ± 9.8	
154344.5-335834		15:43:44.5	-33:58:34	113-183752	-43.9 ± 1.6	-11.5 ± 1.6	
Lupus 3 cloud							
160539.8-384811		16:05:39.8	-38:48:11	103-200987	168.8 ± 6.9	-27.3 ± 7.5	1, 2
160752.3-385806	Sz 95	16:07:52.3	-38:58:06	103-202637	16.8 ± 8.4	-49.4 ± 15.3	
160908.5-390213		16:09:08.5	-39:02:13	102-194972	-40.2 ± 8.3	-62.1 ± 3.2	
161001.1-384315		16:10:01.1	-38:43:15	103-203772	22.7 ± 2.9	19.8 ± 2.8	
Lupus 4 cloud							
160111.6-413730		16:01:11.6	-41:37:30	097-208263	76.9 ± 28.2	50.0 ± 29.5	1

Notes.

(1) Wrong UCAC3 proper motion.

(2) This source has a reported visual companion without UCAC3 counterpart.

- Kraus, A. L. & Hillenbrand, L. A. 2007, AJ 134, 2340
Krautter, J. 1991, in Reipurth, B. (Ed.): *Low-Mass Star Formation in Southern Molecular Clouds*, ESO Scientific Report 11, 127
Krautter, J., Wichmann, R., Schmitt J. H. M. M. et al. 1997, A&AS 123, 329
Kroupa, P. & Bouvier, J. 2003, MNRAS 346, 369
López Martí, B., Eisloffel, J. & Mundt, R. 2005, A&A 440, 139
Luhman, K. L., Stauffer, J. R., Muench, A. A., et al. 2003, ApJ 593, 1093
Mamajek, E. E. 2009, in: *Exoplanets and disks: Their formation and diversity*, AIP Conference Proceedings, Volume 1158, p.3
Maxted, P. F. L., Jeffries, R. D., Oliveira, J. M. et al. 2008, MNRAS 385, 2210
Merín, B., Jørgensen, J., Spezzi, L. et al. 2008, ApJS 177, 551
Monet, D. G., Levine, S. E., Canzian, B. et al. 2003, AJ 125, 984
Morau, E., Bouvier, J. & Stauffer, J. 2001, A&A 367, 211
Nakajima, Y., Tamura, M., Oasa, Y. & Nakajima, T. 2000, ApJ 119, 873
Pöppel, W. G. L. 1997, Fund. Cosm. Phys. 18, 1
Reipurth, B. & Zinnecker, H. 1993, A&A 278, 81
Röser, S., Schilbach, E., Schwan, H. et al. 2008, A&A 488, 401
Schlegel, D. J., Finkbeiner, D. P. & Davis, M. 1998, ApJ 500, 525
Schwartz, R. D. 1977, ApJS 35, 161
Skrutskie, M. F., Cutri, R. M., Stiening, R. et al. 2006, AJ, 131,1163
Tachihara, K., Dobashi, K., Mizuno, A. et al. 1996, PASJ 48, 489
Tachihara, K., Toyoda, S., Onishi, T. et al. 2001, PASJ 53, 1081
Urban, S. E., Corbin, T. E., Wycoff, G. L. et al. 1998, AJ, 115, 1212
Wichmann, R., Krautter, J., Covino, E. et al. 1997, A&A 320, 185 (Wichmann et al. 1997a)
Wichmann, R., Sterzik, M., Krautter, J. et al. 1997, A&A 326, 211 (Wichmann et al. 1997b)
Zacharias, N., Finch, C., Girard, T. et al. 2010, AJ 139, 2184

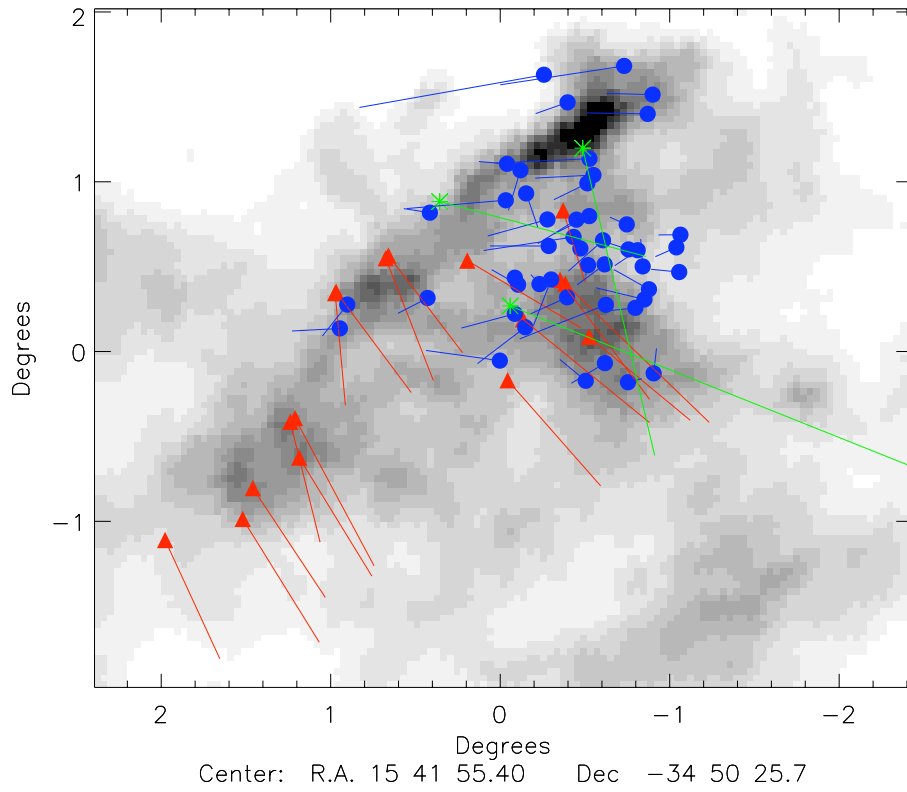


Fig. 2. Current spatial location of the Lupus sources from our UCAC3 sample in Lupus 1. Group A sources are indicated with red triangles, Group B sources with blue circles and outliers with green asterisks. The lines show the expected displacement of these objects within 10^5 Myr. The background image is a SFD dust map (Schlegel et al. 1998) showing the location of the cloud cores.

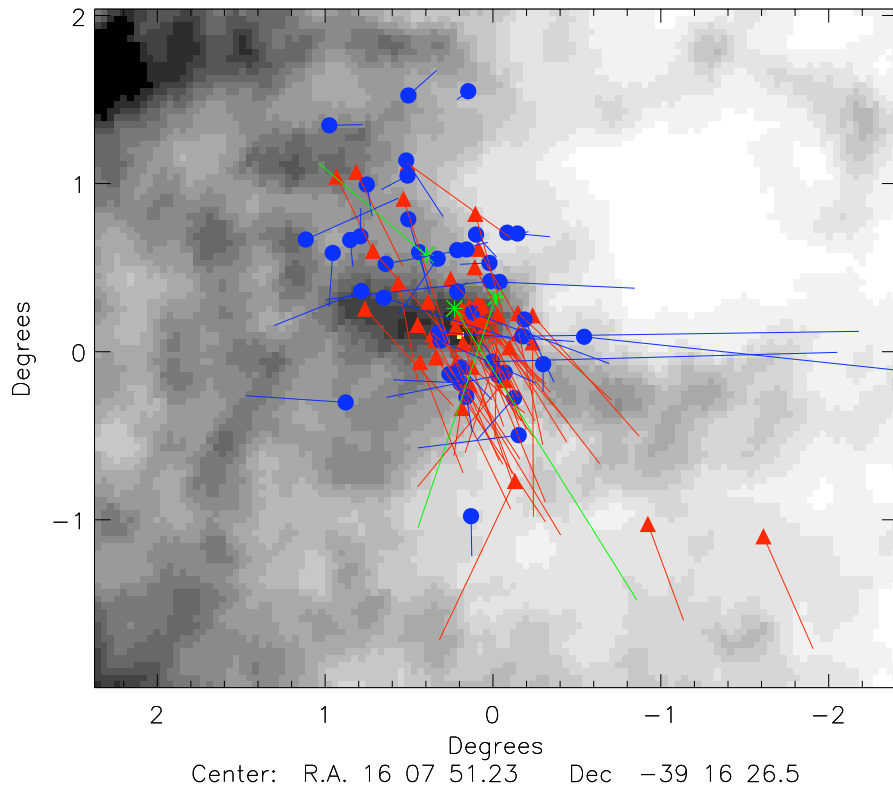


Fig. 3. Same as Fig. 2 for Lupus 3.

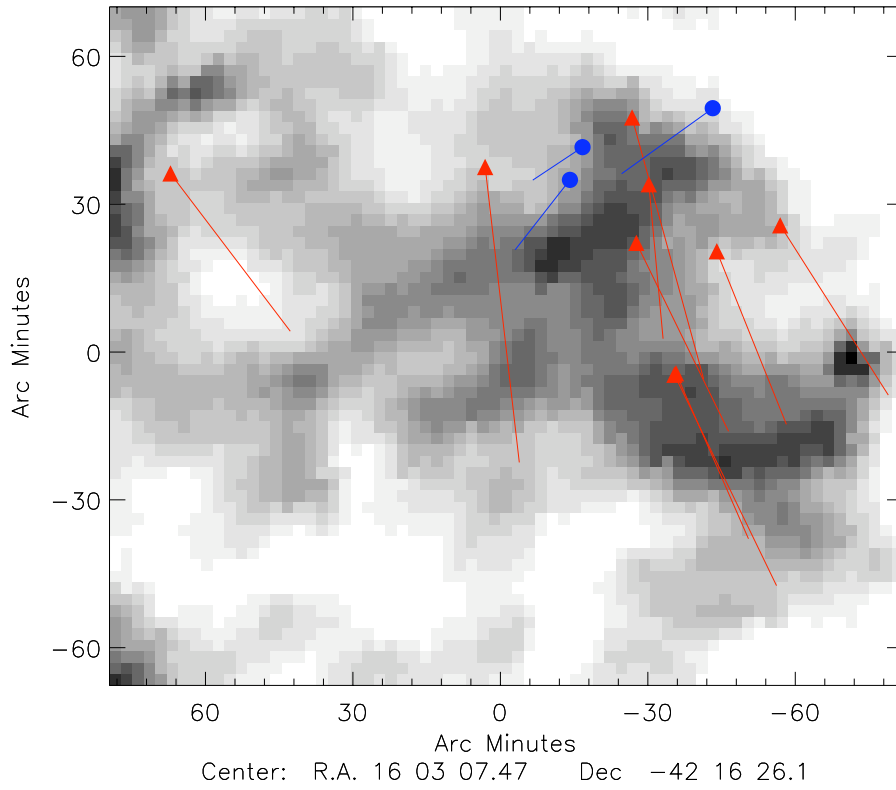


Fig. 4. Same as Fig. 2 for Lupus 4.

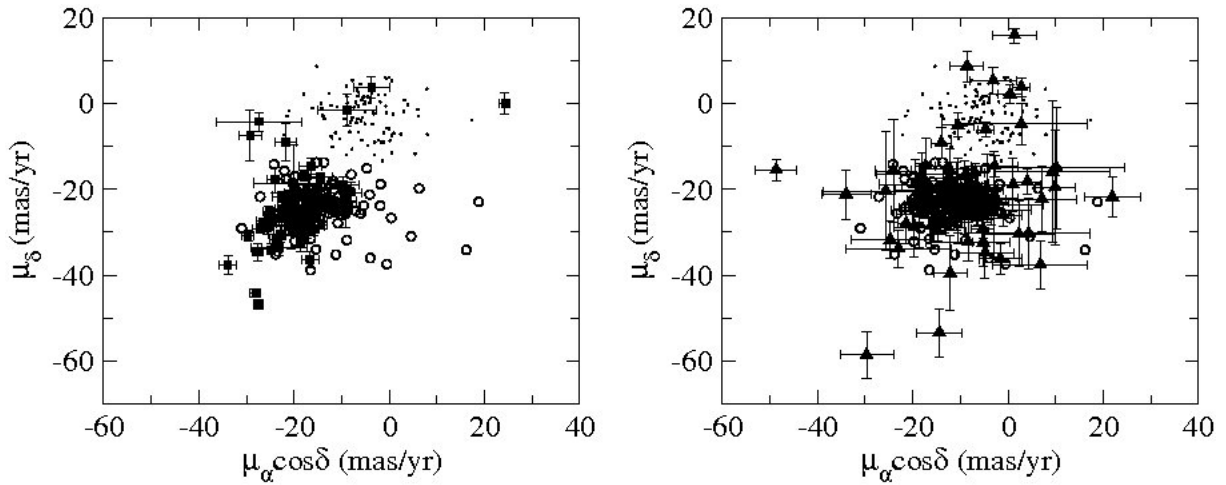


Fig. 6. Comparison of proper motion components of the Group A and Group B sources (open circles and dots, respectively) with those of other Gould Belt populations: Lupus ROSAT stars (filled squares, left panel) and Upper Scorpius members (filled triangles, right panel).

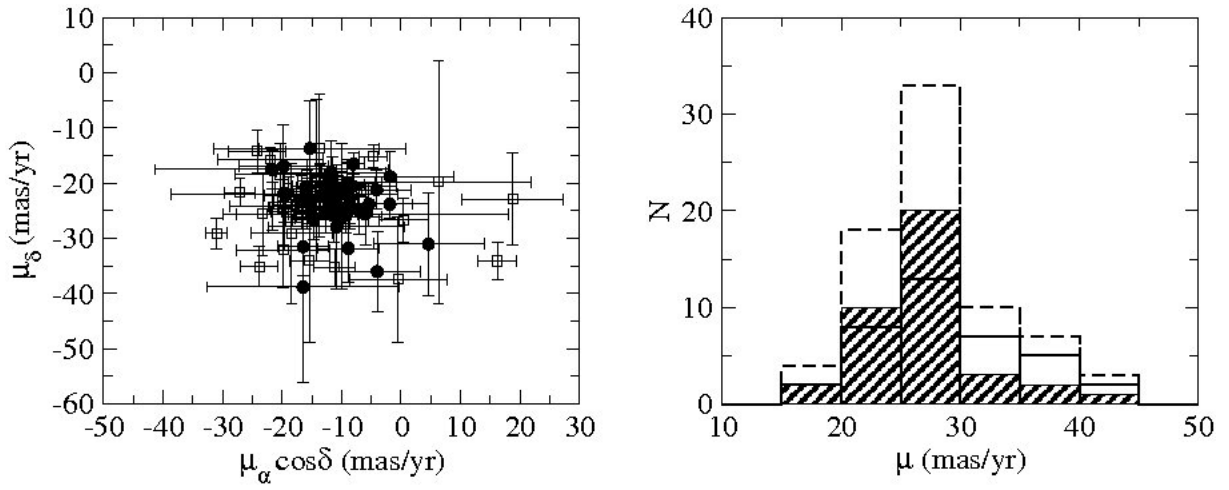


Fig. 7. *Left panel:* Vector point diagrams for the Lupus kinematic members (our Group A). Class I/II sources are marked with filled circles, class III sources with open squares. *Right panel:* Proper motion distribution for the whole sample (dashed histogram) and for the class I/II and class III sources separately (hashed and blank histogram, respectively).

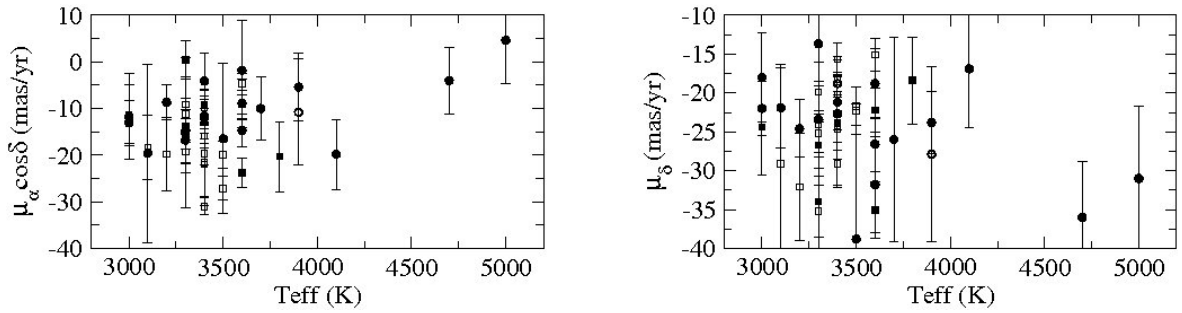


Fig. 8. Proper motion components of our Lupus kinematic members plotted against effective temperature. Solid and open symbols stand for objects with and without spectroscopic confirmation of youth, respectively. Class II and class III sources are indicated with circles and squares, respectively.

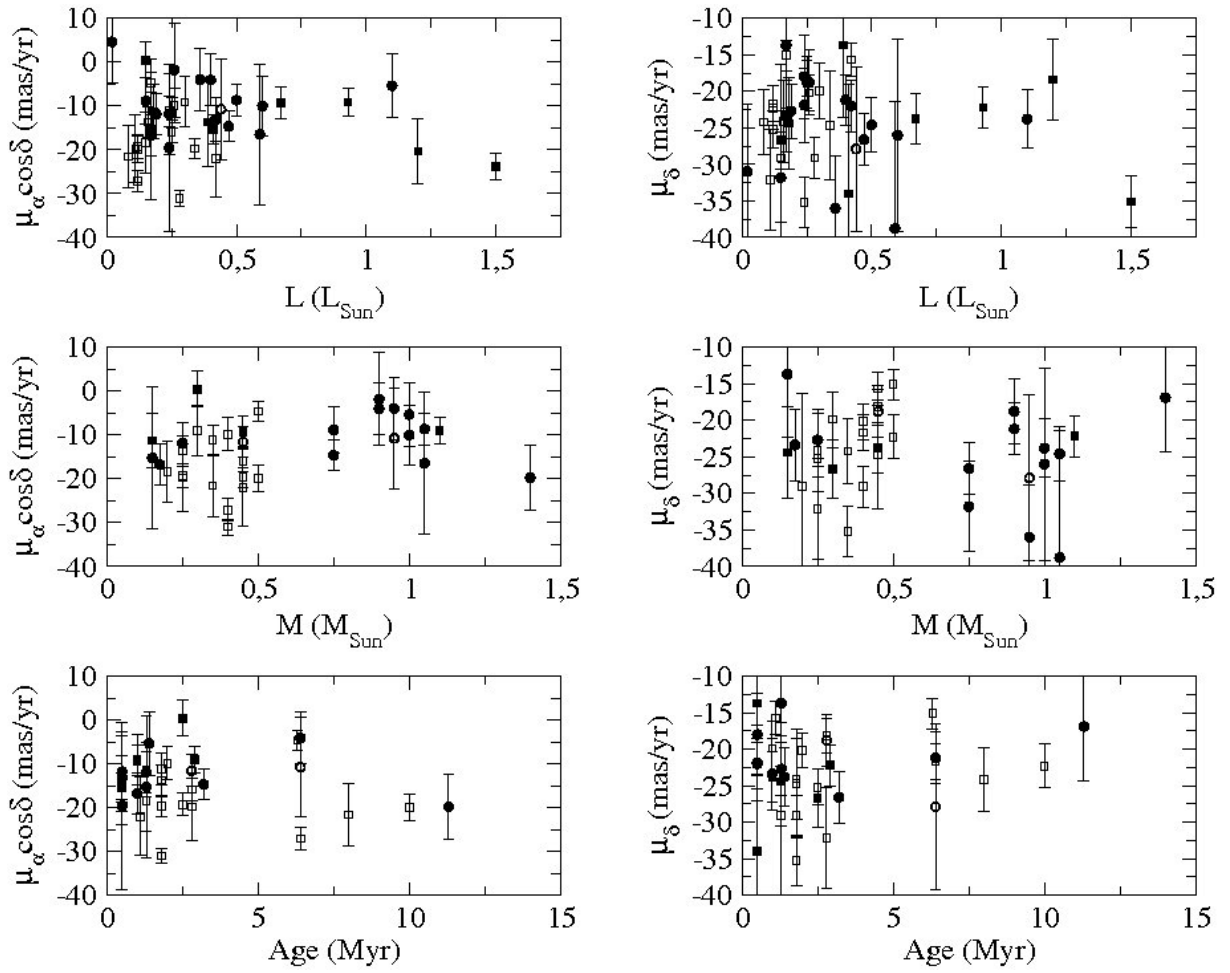


Fig. 9. Proper motion components of the Lupus kinematic members plotted against luminosity, mass and age of the objects (upper, middle and lower panels, respectively). Symbols as in Fig. 8

Group A sources (Lupus kinematic members)

SSTc2d J	Other names	α (J2000)	δ (J2000)	UCAC3	$\mu_\alpha \cos \delta$ (mas/yr)	μ_δ (mas/yr)	Notes
Lupus 1 Cloud							
153805.7-341535		15:38:05.7	-34:15:35	112-181227	-5.6 ± 1.5	-3.3 ± 1.4	
153905.2-341210		15:39:05.2	-34:12:10	112-181437	-8.3 ± 2.1	-6.6 ± 2.3	
153927.8-344617	Sz 65, IK Lup	15:39:27.9	-34:46:17	111-179766	-21.7 ± 19.6	-17.5 ± 3.5	
154009.4-342734		15:40:09.4	-34:27:34	112-181631	-31.0 ± 1.8	-29.1 ± 2.8	
154013.7-340142		15:40:13.7	-34:01:42	112-181650	-4.7 ± 2.3	-15.1 ± 2.1	1
154018.5-342614		15:40:18.5	-34:26:14	112-181670	-19.3 ± 2.6	-25.2 ± 2.5	
154122.0-344015		15:41:22.0	-34:40:15	111-180007	-27.1 ± 2.5	-21.7 ± 2.5	
154148.3-350145		15:41:48.3	-35:01:45	110-180365	-19.9 ± 3.0	-22.3 ± 3.0	
154201.8-345449		15:42:01.8	-34:54:49	111-180129	-17.9 ± 2.2	2.2 ± 2.2	
154257.6-341928		15:42:57.6	-34:19:28	112-182163	-24.2 ± 4.8	-14.2 ± 3.9	
154344.5-335834		15:43:44.5	-33:58:34	113-183752	-43.9 ± 1.6	-11.5 ± 1.6	
154512.9-341731	Sz 68, HT Lup	15:45:12.9	-34:17:31	112-182463	-15.7 ± 1.8	-20.7 ± 1.2	2
154517.4-341829	Sz 69, HW Lup	15:45:17.4	-34:18:28	112-182467	-10.0 ± 6.8	-26.0 ± 13.2	2
	Sz 70	15:46:43.0	-34:30:12	111-181035	-15.8 ± 4.5	-21.5 ± 3.9	
	Sz 71	15:46:44.7	-34:30:35	111-181040	-1.9 ± 6.5	-23.8 ± 2.5	
	Sz 72	15:47:50.6	-35:28:35	110-181840	-15.2 ± 2.5	-25.3 ± 2.5	
	Sz 73	15:47:56.9	-35:14:35	110-181858	-16.5 ± 4.2	-31.5 ± 5.3	
	Sz 74	15:48:05.2	-35:15:53	110-181875	-6.0 ± 24.0	-25.6 ± 5.5	2
	Sz 75	15:49:12.1	-35:39:04	109-183258	-15.1 ± 2.8	-23.4 ± 2.5	
	Sz 76	15:49:30.8	-35:49:52	109-183338	-15.9 ± 2.0	-26.4 ± 2.0	
	Sz 77	15:51:47.0	-35:56:43	109-183891	-11.1 ± 2.1	-25.4 ± 1.4	2
Lupus 3 Cloud							
	RY Lup	15:59:28.4	-40:21:51	100-186413	-11.4 ± 1.3	-23.7 ± 1.2	
	EX Lup	16:03:05.5	-40:18:26	100-188355	-8.1 ± 7.4	-20.5 ± 3.3	
	Sz 86	16:06:44.3	-39:14:11	102-194310	-0.5 ± 8.2	-37.4 ± 11.4	
160644.6-390432		16:06:44.6	-39:04:32	102-194315	-23.3 ± 4.3	-25.6 ± 7.6	
160710.1-391104	Sz 90	16:07:10.1	-39:11:03	102-194459	-5.4 ± 7.3	-23.8 ± 4.0	
160711.6-390348	Sz 91	16:07:11.6	-39:03:48	102-194468	-20.3 ± 7.5	-18.4 ± 5.6	3
160715.2-400342	Sz 92, Th 22	16:07:15.2	-40:03:42	100-191044	16.2 ± 3.2	-34.1 ± 3.3	
160727.1-391601		16:07:27.1	-39:16:01	102-194531	-19.7 ± 2.3	-24.7 ± 7.4	
160734.3-392742		16:07:34.3	-39:27:42	102-194554	18.8 ± 8.5	-22.9 ± 8.3	
160749.6-390429	Sz 94	16:07:49.6	-39:04:29	102-194608	0.4 ± 4.1	-26.7 ± 4.0	
160754.1-392046		16:07:54.1	-39:20:46	102-194634	6.3 ± 15.6	-19.8 ± 22.0	1
160758.7-392109		16:07:58.7	-39:21:09	102-194657	7.9 ± 11.3	3.4 ± 9.4	
160812.6-390834	Sz 96	16:08:12.6	-39:08:33	102-194723	-9.1 ± 3.1	-22.2 ± 2.8	
160817.4-390105		16:08:17.4	-39:01:05	102-194744	-18.4 ± 6.9	-29.1 ± 12.7	
160821.8-390422	Sz 97, Th 24	16:08:21.8	-39:04:21	102-194777	-11.9 ± 4.6	-22.7 ± 3.7	
160822.5-390446	Sz 98, HK Lup	16:08:22.5	-39:04:46	102-194779	-8.7 ± 3.6	-23.8 ± 3.4	
160822.8-390058		16:08:22.8	-39:00:58	102-194781	-11.6 ± 3.6	-18.8 ± 3.5	
160825.2-384055		16:08:25.2	-38:40:55	103-203004	-13.7 ± 3.5	-24.1 ± 5.6	
160825.8-390601	Sz 100, Th 26	16:08:25.8	-39:06:01	102-194798	-19.6 ± 19.1	-21.9 ± 5.1	2
160827.8-390040		16:08:27.8	-39:00:40	102-194810	-9.1 ± 5.8	-19.9 ± 3.8	
160828.4-390532	Sz 101, Th 27	16:08:28.4	-39:05:32	102-194814	-13.7 ± 10.1	-13.7 ± 9.8	1
160829.7-390311	Sz 102, Krautter's star	16:08:29.7	-39:03:11	102-194820	4.6 ± 9.3	-31.0 ± 9.3	
160830.3-390611	Sz 103, Th 29	16:08:30.3	-39:06:11	102-194825	-15.3 ± 16.1	-13.7 ± 8.6	1
160830.7-382827		16:08:30.7	-38:28:27	104-202988	-7.0 ± 2.1	-25.0 ± 4.3	
160831.6-384729		16:08:31.6	-38:47:29	103-203065	-12.3 ± 6.7	-22.4 ± 3.0	
160836.2-392302		16:08:36.2	-39:23:02	102-194850	-9.2 ± 3.6	-25.7 ± 3.2	
160839.8-390625	Sz 106	16:08:39.8	-39:06:25	102-194868	-16.5 ± 16.1	-38.8 ± 17.4	
160839.8-392922		16:08:39.8	-39:29:22	102-194869	-19.8 ± 7.8	-32.1 ± 6.9	
160841.8-390137	Sz 107	16:08:41.8	-39:01:37	102-194875	-11.3 ± 6.3	-24.4 ± 6.2	
160851.6-390318	Sz 110, Th 32	16:08:51.6	-39:03:18	102-194906	-8.7 ± 3.7	-24.6 ± 3.7	
160853.2-391440	2MASS J16085324-3914401	16:08:53.2	-39:14:40	102-194910	-10.8 ± 11.4	-27.9 ± 11.3	
160854.7-393744	Sz 111, Th 33	16:08:54.7	-39:37:44	101-192059	-10.6 ± 3.1	-21.6 ± 3.1	
160855.5-390234	Sz 112	16:08:55.5	-39:02:34	102-194917	-11.8 ± 9.2	-18.0 ± 5.7	2
160901.8-390513	Sz 114, V908 Sco	16:09:01.8	-39:05:12	102-194945	-13.1 ± 4.9	-22.0 ± 3.5	
160904.6-392112		16:09:04.6	-39:21:12	102-194958	-13.7 ± 3.8	-20.8 ± 4.1	

Table 2: continued.

SSTc2d J	Other names	α (J2000)	δ (J2000)	UCAC3	$\mu_\alpha \cos \delta$ (mas/yr)	μ_δ (mas/yr)	Notes
160906.2-390852	Sz 115	16:09:06.2	-39:08:52	102-194964	-16.8 ± 4.7	-23.4 ± 4.9	
160915.7-385139		16:09:15.7	-38:51:39	103-203455	-21.6 ± 7.2	-24.2 ± 4.4	
160937.4-391044		16:09:37.4	-39:10:44	102-195079	-3.4 ± 3.7	-1.8 ± 3.3	
160942.6-391941	Sz 116, Th 36	16:09:42.6	-39:19:41	102-195093	-23.8 ± 3.1	-35.1 ± 3.6	2
160944.3-391330	Sz 117, Th 37	16:09:44.3	-39:13:30	102-195097	-14.7 ± 3.5	-26.6 ± 3.5	
160948.6-391117	Sz 118	16:09:48.6	-39:11:17	102-195106	-19.8 ± 7.5	-16.9 ± 7.5	
160957.1-385948	Sz 119	16:09:57.1	-38:59:48	103-203753	-15.4 ± 3.3	-34.0 ± 14.9	
161012.2-392118	Sz 121, Th 40	16:10:12.2	-39:21:18	102-195162	-9.3 ± 3.5	-23.8 ± 3.5	
161016.4-390805	Sz 122, Th 41	16:10:16.4	-39:08:05	102-195173	-17.6 ± 3.2	-24.0 ± 3.0	
161034.3-381031		16:10:34.3	-38:10:31	104-203985	-22.0 ± 8.9	-15.7 ± 2.2	
161041.9-382304		16:10:41.9	-38:23:04	104-204037	-11.2 ± 3.5	-35.2 ± 3.4	
161051.6-385314	Sz 123, Th 42	16:10:51.6	-38:53:14	103-204003	-4.1 ± 5.9	-21.2 ± 3.5	2
161118.7-385824		16:11:18.7	-38:58:24	103-204143	-11.9 ± 3.9	-10.1 ± 2.9	
161138.1-384135		16:11:38.1	-38:41:35	103-204233	-15.9 ± 2.6	-18.2 ± 2.4	
161153.4-390216	Sz 124, Th 43	16:11:53.3	-39:02:16	102-195419	-19.0 ± 2.1	-20.9 ± 2.1	
161207.6-381324		16:12:07.6	-38:13:24	104-204340	-9.9 ± 3.8	-20.2 ± 2.4	
161243.8-381503		16:12:43.7	-38:15:03	104-204438	-8.0 ± 1.9	-16.5 ± 1.9	1
Lupus 4 Cloud							
	Sz 128	15:58:07.4	-41:51:48	097-206859	-13.5 ± 4.8	-20.5 ± 4.1	
	Sz 129	15:59:16.5	-41:57:09	097-207576	-8.7 ± 2.1	-21.0 ± 2.1	
160000.6-422158		16:00:00.6	-42:21:57	096-205744	-9.0 ± 4.6	-20.1 ± 4.5	2
160002.4-422216		16:00:02.4	-42:22:15	096-205752	-12.7 ± 5.4	-25.6 ± 3.4	2
160031.1-414337	Sz 130	16:00:31.0	-41:43:37	097-208086	-1.8 ± 10.7	-18.8 ± 4.5	1, 2
160044.5-415531	MY Lup, IRAS 15573-4147	16:00:44.5	-41:55:31	097-208155	-11.4 ± 4.3	-22.9 ± 2.0	
160049.4-413004	Sz 131	16:00:49.4	-41:30:04	097-208172	-8.9 ± 5.2	-31.8 ± 6.2	
160329.4-414003	Sz 133	16:03:29.4	-41:40:03	097-208899	-4.0 ± 7.2	-36.0 ± 7.2	2
	Sz 134	16:09:12.2	-41:40:25	097-211385	-14.3 ± 3.0	-19.5 ± 14.7	

Notes.

(1) Ambiguous source (it could belong to either group).

(2) This source has a reported visual companion without UCAC3 counterpart.

(3) Reported visual companion (Ghez et al. 1997, $\sim 8.9''$) with UCAC3 counterpart.

SSTc2d J	Other names	α (J2000)	δ (J2000)	UCAC3	$\mu_\alpha \cos \delta$ (mas/yr)	μ_δ (mas/yr)	Notes
Lupus 1 Cloud							
153652.8-340956		15:36:52.8	-34:09:56	112-180962	-5.2 ± 1.7	-0.1 ± 1.7	
153654.1-342307		15:36:54.1	-34:23:07	112-180966	-7.1 ± 1.8	0.5 ± 1.8	
153659.4-341425		15:36:59.4	-34:14:25	112-180979	-5.1 ± 1.6	-2.0 ± 1.6	
153736.0-345902		15:37:36.0	-34:59:02	111-179553	0.6 ± 1.7	5.3 ± 1.7	
153742.9-332034		15:37:42.9	-33:20:34	114-181267	-4.1 ± 1.4	0.2 ± 1.4	
153745.7-342920		15:37:45.7	-34:29:20	112-181159	-9.0 ± 1.1	4.1 ± 1.1	
153750.9-332722		15:37:50.9	-33:27:22	114-181289	-7.0 ± 1.7	0.1 ± 1.7	
153753.2-343256		15:37:53.2	-34:32:56	111-179602	-12.6 ± 1.8	2.4 ± 1.8	
153756.8-342117		15:37:56.8	-34:21:17	112-181197	-0.6 ± 1.7	5.8 ± 2.1	
153805.7-341535		15:38:05.7	-34:15:35	112-181227	-5.6 ± 1.5	-3.3 ± 1.4	
153808.7-343557		15:38:08.7	-34:35:57	111-179635	-6.5 ± 1.7	-0.6 ± 1.7	
153820.2-350215		15:38:20.2	-35:02:15	110-179447	3.2 ± 1.6	0.8 ± 1.7	
153821.4-341519		15:38:21.4	-34:15:19	112-181280	-6.6 ± 3.5	1.8 ± 3.6	
153824.8-340629		15:38:24.8	-34:06:29	112-181300	-3.9 ± 1.6	1.5 ± 2.9	
153831.6-331031		15:38:31.6	-33:10:31	114-181385	-5.9 ± 1.8	-4.1 ± 1.8	
153859.5-343458		15:38:59.5	-34:34:58	111-179723	-22.2 ± 1.5	-7.3 ± 1.5	1
153900.3-345534		15:39:00.3	-34:55:34	111-179724	-8.1 ± 2.0	-4.3 ± 2.0	
153902.1-342040		15:39:02.1	-34:20:40	112-181429	-6.9 ± 2.3	-4.4 ± 2.3	
153905.2-341210		15:39:05.2	-34:12:10	112-181437	-8.3 ± 2.1	-6.6 ± 2.3	
153922.3-334909		15:39:22.3	-33:49:09	113-182842	-11.0 ± 2.3	-0.7 ± 2.3	
153929.0-340339		15:39:29.0	-34:03:39	112-181511	-7.9 ± 2.3	-3.8 ± 2.3	
153929.2-334322		15:39:29.2	-33:43:22	113-182854	-16.1 ± 3.1	-1.0 ± 2.3	
153930.5-342058		15:39:30.5	-34:20:58	112-181518	-0.6 ± 2.0	-2.2 ± 2.0	
153932.6-335205		15:39:32.6	-33:52:05	113-182872	-6.6 ± 2.3	-3.5 ± 2.3	
153933.2-350151		15:39:33.2	-35:01:51	110-179659	-6.0 ± 4.5	4.5 ± 2.4	
153943.8-341506		15:39:43.8	-34:15:06	112-181558	-3.7 ± 1.7	2.4 ± 1.7	
153950.8-340456		15:39:50.8	-34:04:56	112-181575	-8.8 ± 2.5	-5.1 ± 2.5	
153955.6-341103		15:39:55.6	-34:11:03	112-181587	-21.5 ± 2.3	-2.9 ± 2.3	
154006.1-343224		15:40:06.1	-34:32:24	111-179825	-9.4 ± 2.7	-3.5 ± 2.4	
154006.9-332331		15:40:06.9	-33:23:31	114-181587	-3.2 ± 2.7	-2.4 ± 2.4	
154013.7-340142		15:40:13.7	-34:01:42	112-181650	-4.7 ± 2.3	-15.1 ± 2.1	
154033.8-342607		15:40:33.8	-34:26:07	112-181729	-4.5 ± 1.7	-9.8 ± 1.6	
154038.1-341417		15:40:38.1	-34:14:17	112-181753	-14.3 ± 8.6	0.0 ± 2.5	
154040.4-340455		15:40:40.4	-34:04:55	112-181764	-13.6 ± 1.8	-3.5 ± 1.4	
154047.2-331347		15:40:47.2	-33:13:47	114-181775	-11.3 ± 3.2	-6.8 ± 1.7	
154053.7-342745		15:40:53.7	-34:27:45	112-181810	-2.2 ± 2.8	2.0 ± 2.3	
154116.9-335544		15:41:16.9	-33:55:44	113-183184	2.4 ± 2.3	-7.1 ± 2.3	
154118.0-344301		15:41:18.0	-34:43:01	111-179990	-12.2 ± 1.9	-7.7 ± 1.9	1
154126.7-334732		15:41:26.7	-33:47:32	113-183205	-2.2 ± 2.0	-8.5 ± 2.0	
154130.4-342759		15:41:30.4	-34:27:59	112-181935	-6.8 ± 2.2	3.2 ± 2.2	
154136.0-342532		15:41:36.0	-34:25:32	112-181963	-0.7 ± 2.4	-0.6 ± 2.4	
154136.0-343818		15:41:36.0	-34:38:18	111-180053	-13.8 ± 1.9	-3.0 ± 1.9	
154149.5-334517		15:41:49.5	-33:45:17	113-183262	-5.0 ± 2.5	0.5 ± 2.4	
154151.7-335809		15:41:51.7	-33:58:09	113-183268	-21.1 ± 2.6	-1.7 ± 1.7	
154201.8-345449		15:42:01.8	-34:54:49	111-180129	-17.9 ± 2.2	2.2 ± 2.2	
154344.5-335834		15:43:44.5	-33:58:34	113-183752	-43.9 ± 1.6	-11.5 ± 1.6	
154401.4-340229		15:44:01.4	-34:02:29	112-182317	-5.8 ± 2.3	0.9 ± 2.3	
154406.0-343238		15:44:06.0	-34:32:38	111-180557	-7.7 ± 2.6	-3.2 ± 2.5	
154624.2-343443		15:46:24.2	-34:34:43	111-180973	-6.5 ± 4.4	-6.6 ± 2.3	
154637.4-344307		15:46:37.4	-34:43:07	111-181011	-12.2 ± 5.7	-0.4 ± 3.1	
Lupus 3 Cloud							
160509.3-391203		16:05:09.3	-39:12:03	102-193467	-10.4 ± 7.5	-8.2 ± 3.1	
160624.4-392158		16:06:24.4	-39:21:58	102-194148	0.0 ± 2.8	-5.9 ± 2.8	
160659.5-390605		16:06:59.5	-39:06:05	102-194390	-1.4 ± 2.8	-13.4 ± 5.7	1
160702.6-391203		16:07:02.6	-39:12:03	102-194415	-6.4 ± 3.2	2.6 ± 3.2	
160708.6-394723		16:07:08.6	-39:47:23	101-190770	-14.0 ± 5.4	-2.8 ± 3.3	2
160713.5-383525		16:07:13.5	-38:35:25	103-202192	-1.9 ± 17.8	0.4 ± 4.6	

e 3: continued.

SSTc2d J	Other names	α (J2000)	δ (J2000)	UCAC3	$\mu_\alpha \cos \delta$ (mas/yr)	μ_δ (mas/yr)	Notes
	Sz 93	16:07:17.8	-39:34:05	101-190887	-3.0 ± 2.7	-9.0 ± 2.7	
160732.3-383508		16:07:32.3	-38:35:08	103-202425	-7.4 ± 3.3	-0.8 ± 3.3	
160734.3-392742		16:07:34.3	-39:27:42	102-194554	18.8 ± 8.5	-22.9 ± 8.3	
160735.3-392507		16:07:35.3	-39:25:07	102-194557	-0.9 ± 3.6	6.1 ± 5.1	
160745.9-385245		16:07:45.9	-38:52:45	103-202567	-14.2 ± 7.2	-1.0 ± 6.6	
160747.4-392606		16:07:47.4	-39:26:06	102-194597	-5.1 ± 2.7	-4.7 ± 4.0	
160758.7-392109		16:07:58.7	-39:21:09	102-194657	7.9 ± 11.3	3.4 ± 9.4	
160803.0-385229		16:08:03.0	-38:52:29	103-202756	17.4 ± 3.3	-3.8 ± 3.3	2
160804.6-384558		16:08:04.6	-38:45:58	103-202775	3.9 ± 2.4	-0.3 ± 2.4	
160829.3-383551		16:08:29.3	-38:35:51	103-203038	-3.5 ± 8.6	-4.8 ± 7.8	
160835.5-390035	Par-Lup3-2	16:08:35.5	-39:00:35	102-194847	-7.8 ± 5.7	-10.6 ± 7.5	1
	Sz 105	16:08:37.0	-40:16:21	100-192100	0.2 ± 6.9	-8.6 ± 3.7	3
160844.3-374443		16:08:44.3	-37:44:43	105-204594	3.1 ± 1.4	-1.8 ± 1.4	
160846.4-393347		16:08:46.4	-39:33:47	101-191965	0.5 ± 15.6	-7.5 ± 6.2	
160846.6-384112		16:08:46.6	-38:41:12	103-203212	6.0 ± 9.2	-1.4 ± 3.6	
160855.6-392316		16:08:55.6	-39:23:16	102-194918	1.0 ± 11.4	-6.9 ± 4.1	
160857.3-392849		16:08:57.3	-39:28:49	102-194927	-3.9 ± 3.1	0.7 ± 3.1	
160903.7-385610		16:09:03.7	-38:56:10	103-203354	-0.9 ± 3.4	2.0 ± 2.8	
160903.8-384126		16:09:03.8	-38:41:26	103-203355	-4.6 ± 3.5	1.7 ± 2.6	
160917.6-392537		16:09:17.6	-39:25:37	102-195004	0.8 ± 3.0	-2.5 ± 2.8	
160934.1-391342		16:09:34.1	-39:13:42	102-195072	-1.1 ± 5.6	-9.0 ± 5.6	1
160937.4-391044		16:09:37.4	-39:10:44	102-195079	-3.4 ± 3.7	-1.8 ± 3.3	
160939.5-384431		16:09:39.5	-38:44:31	103-203637	5.4 ± 7.9	-11.7 ± 6.1	1
161013.5-384208		16:10:13.5	-38:42:08	103-203833	-1.6 ± 3.2	-9.0 ± 2.7	1
161032.6-374615	IRAS 16072-3738	16:10:32.6	-37:46:15	105-205237	-7.7 ± 6.8	5.4 ± 3.2	
161033.2-383023		16:10:33.2	-38:30:23	103-203926	-3.1 ± 6.5	-12.0 ± 8.3	1
161034.5-381450		16:10:34.5	-38:14:50	104-203987	6.1 ± 3.0	-3.0 ± 7.6	
161036.7-380927		16:10:36.7	-38:09:27	104-204003	-9.0 ± 1.4	-12.0 ± 2.4	1
161114.8-384618		16:11:14.8	-38:46:18	103-204118	-5.4 ± 6.1	1.6 ± 2.5	
161118.7-385824		16:11:18.7	-38:58:24	103-204143	-11.9 ± 3.9	-10.1 ± 2.9	1, 2
161148.7-381758		16:11:48.7	-38:17:58	104-204298	-1.2 ± 6.1	-6.8 ± 15.5	
161200.1-385557		16:12:00.1	-38:55:57	103-204299	8.0 ± 18.5	-7.2 ± 4.8	2
161200.9-383625		16:12:00.9	-38:36:25	103-204302	-0.1 ± 4.2	6.1 ± 2.3	
161219.6-383742		16:12:19.6	-38:37:42	103-204359	-0.4 ± 8.6	-5.7 ± 3.3	
	Sz 125	16:12:30.1	-39:35:40	101-193738	-8.9 ± 3.5	1.7 ± 2.4	
161251.7-384216		16:12:51.7	-38:42:16	103-204499	0.6 ± 3.1	-11.5 ± 8.1	1
161256.0-375643		16:12:56.0	-37:56:44	105-205869	-8.8 ± 10.4	0.1 ± 4.0	
161341.0-383724		16:13:40.9	-38:37:24	103-204732	-15.3 ± 10.4	8.7 ± 7.5	
Lupus 4 Cloud							
155921.8-412808		15:59:21.8	-41:28:08	098-201434	-12.0 ± 5.6	-8.0 ± 2.8	
160143.3-413606		16:01:43.3	-41:36:06	097-208357	-5.9 ± 12.0	-4.0 ± 5.6	
160157.0-414244	IRAS 15585-4134	16:01:57.0	-41:42:44	097-208409	-5.8 ± 4.7	-8.5 ± 4.6	1

Notes.

- (1) Ambiguous source (it could belong to either group).
- (2) This source has a reported visual companion without UCAC3 counterpart.
- (3) Reported visual companion (Ghez et al. 1997, $\sim 10''$) with UCAC3 counterpart.